JOC Article

Efficient Fluoride-Selective Fluorescent Host: Experiment and Theory†

Jin Yong Lee,*,‡ Eun Jin Cho,‡ Shaul Mukamel,§ and Kye Chun Nam*,‡

Department of Chemistry, Chonnam National University, 300 Yongbong-Dong, Bugku, Gwangju, 500-757, Korea, and Department of Chemistry, University of California, Irvine, Irvine, California 92697

jinyong@chonnam.ac.kr; kcnam@chonnam.ac.kr

Received November 9, 2003

A new naphthalene derivative containing a urea group at the 1,8-position of naphthalene was synthesized and showed a unique absorption and fluorescence peak with fluoride ion. Calculations suggested that a new peak was attributed to the increased anionic character of urea nitrogen due to the strongly charged hydrogen bonding between fluoride and amide protons of the urea. The fluoride selectivity among halides (F^-, Cl^-, Br^-) comes from the fact that the fluoride approaches much closer to the amide protons than other halides and resides in the cavity with fast dynamics. The nature of electronic transitions that were analyzed from the calculations by the collective electronic oscillator method also supports the anionic nature of the complex between host and fluoride.

Introduction

The development of new receptors capable of recognizing neutral and charged species has attracted considerable interest in the recent past.[1−3] Despite that cation receptors have been studied for more than four decades, the design of anion receptors has received much less attention comparitively.[4−6] This may be because concentrations of negative potential are more accessible and manageable on the molecular scale than those of positive potential; hence, it is easier to design a molecular system to recognize positively charged species. Water-soluble anions such as fluoride, chloride, phosphate, and carboxylate play crucial roles in a range of biological phenomena and are implicated in many disease states.[7] In particular, we have long been interested in fluoride because of its beneficial effects in human physiology such as prevention of dental caries[8] and treatment of osteoporosis,[9] etc.

Sessler and collaborators focused on the use of pyrrole-based anion recognition motifs and developed several functionalized calixpyrrole and dipyrrolylquinoxaline

* Corresponding authors. (J.Y.L) Phone: +82-62-530-3384. Fax: +82-62-530-3389.

† This paper is dedicated to professor Dong H. Kim on his 70th birthday.

‡ Chonnam National University.

§ University of California, Irvine.

(1) (a) Atwood, J. L., Davies, J. E. D., MacNicol, D. D., Vögtle, F., Lehn, J.-M., Eds.; *Comprehensive Supramolecular Chemistry*; Elsevier: Amsterdam, 1996; Vols. 1−11. (b) Niikura, K.; Metzger, A.; Anslyn, E. V. *J. Am. Chem. Soc.* **1998**, *120*, 8533. (c) Bission, A. P.; Lynch, V. M.; Mohahan, M.-K. C.; Anslyn, E. V. *Angew. Chem., Int. Ed.* **1997**, *36*, 2340. (d) Gutsche, C. D.; Nam, K. C. *J. Am. Chem. Soc.* **1988**, *110*, 6153. (e) Nam, K. C.; Choi, Y. J.; Kim, D. S.; Kim, J. M.; Chun, J. C. *J. Org. Chem.* **1997**, *62*, 6441. (f) Ko, S. W.; Lee, S. H.; Park, K.; Lee, S. S.; Nam, K. C. *Supramol. Chem.* **2003**, *15*, 117. (g) Oh, H.; Choi, E. M.; Jeong, H.; Nam, K. C.; Jeon, S. *Talanta* **2000**, *53*, 535. (h) Nam, K. C.; Ko, S. W.; Kang, S. O.; Lee, S. H.; Kim, D. S. *J. Inclusion Phenom. Macrocycl. Chem.* **2001**, *40*, 285.

(2) (a) Stack, T. D. P.; Hou, Z.; Raymond, K. N. *J. Am. Chem. Soc.* **1993**, *115*, 6466. (b) Hong, B. H.; Bae, S. C.; Lee, C.-W.; Jeong, S.; Kim, K. S. *Science* **2001**, *294*, 348. (c) De Wall, S. L.; Barbour, L. J.; Gokel, G. W. *J. Am. Chem. Soc.* **1999**, *121*, 8405. (d) Choi, H. S.; Kim, K. S. *Angew. Chem., Int. Ed.* **1999**, *111*, 2400. (e) Wang, J.; Gutsche, C. D. *J. Org. Chem.* **2002**, *67*, 4423.

(3) (a) Kim, H. G.; Lee, C.-W.; Yun, S.; Hong, B. H.; Kim, Y.-O.; Kim, D.; Ihm, H.; Lee, J. W.; Lee, E. C.; Tarakeshwar, P.; Park, S.-M.; Kim, K. S. *Org. Lett.* **2002**, *4*, 3971. (b) Choi, H. S.; Suh, S. B.; Cho, S. J.; Kim, K. S. *Proc. Natl. Acad. Sci. U.S.A.* **1998**, *95*, 12094. (c) Oh, K. S.; Lee, C.-W.; Choi, H. S.; Lee, S. J.; Kim, K. S. *Org. Lett.* **2000**, *2*, 2679. (d) Yun, S.; Kim, Y.-O.; Kim, D.; Kim, H. G.; Ihm, H.; Kim, J. K.; Lee, C.-W.; Lee, W. J.; Yoon, J.; Oh, K. S.; Park, S.-M.; Kim, K. S. *Org. Lett.* **2003**, *5*, 471.

(4) (a) Yun, S.; Ihm, H.; Kim, H. G.; Lee, C.-W.; Indrajit, B.; Oh, K. S.; Gong, Y. J.; Lee, J. W.; Yoon, J.; Lee, H. C.; Kim, K. S. *J. Org. Chem.* **2003**, *68*, 2467. (b) Beer, P. D.; Gale, P. A. *Angew. Chem., Int. Ed.* **2001**, *40*, 486. (c) Antonisse, M. M. G.; Reinhoudt, D. N. *Chem. Commun.* **1998**, 143. (d) Schmidtchen, F. P.; Berger, M. *Chem. Rev.* **1997**, *97*, 1609. (e) Miyaji, H.; Sessler, J. L. *Angew. Chem., Int. Ed.* **2001**, *40*, 154. (f) Yamaguchi, S.; Akiyama, S.; Tamao, K. *J. Am. Chem. Soc.* **2001**, *123*, 11372.

(5) (a) Kim, K. S.; Cui, C.; Cho, S. J. *J. Phys. Chem. B* **1998**, *102*, 461. (b) Yamaguchi, S.; Akiyama, S.; Tamao, K. *J. Am. Chem. Soc.* **2001**, *123*, 11372. (c) Beer, P. D.; Drew, M. G. M.; Hesek, D.; Nam, K. C. *Chem. Commun.* **1997**, 107. (d) Nam, K. C.; Kang, S. O.; Jeong, H. S.; Jeon, S. *Tetrahedron Lett.* **1999**, *40*, 7343. (e) Beer, P. D.; Hesek, D.; Nam, K. C.; Drew, M. G. M. *Organometallics* **1999**, *18*, 3933. (f) Kang, S. O.; Jeon, S.; Nam, K. C. *Supramol. Chem.* **2002**, *14*, 405. (g) Jeong, H. S.; Choi, E. M.; Kang, S. O.; Nam, K. C.; Jeon, S. *J. Electroanal. Chem.* **2000**, *485*, 154.

(6) (a) Han, M. S.; Kim, D. H. *Angew. Chem., Int. Ed.* **2002**, *41*, 3809. (b) Jeon, S.; Lee, H.; Jeong, H.; Oh, J. M.; Nam, K. C. *Electroanal.* **2003**, *5*, 872.

(7) Tomich, J. M.; Wallace, D.; Henderson, K.; Mitchell, K. E.; Radke, G.; Brandt, T.; Ambler, C. A.; Scott, A. J.; Grantham, J.; Sullivan, L.; Iwamoto, T. *Biophys. J.* **1998**, *74*, 256.

(8) Kirk, K. L. *Biochemistry of the Halogens and Inorganic Halides*; Plenum Press: New York, 1991; p 58.

(9) Kleerekoper, M. *Endocrinol. Metab. Clin. North Am.* **1998**, *27*, 441.

10.1021/jo0356457 CCC: $27.50
Published on Web 01/14/2004

receptors.[10−12] Recently, they reported a new efficient fluoride anion receptor based on the metal coordination of fused dipyrrolylquinoxaline derivative.[13] A fluoride-selective binding receptor that has a deep-cavity calix-[4]pyrrole was reported by Woods et al. and found to exclusively bind fluoride ions in DMSO-d_6.[14] This unusual binding results from the favorable electrostatic interactions that the fluoride gains by sitting lower in the phenolic cavity of the receptor. Aromatic rings have abundant π-electrons over the space, in particular, above and below the aromatic plane, which makes aromatic compounds unable to recognize anions. However, the first aromatic receptor based on electron-deficient 1,3,5-triazine, which interacts with fluoride, chloride, and azide anions, was reported.[15] Another strategy for anion recognition is to utilize a functional cavity as proposed by Sato et al.[16] In this category, benzene-based tripodal imidazolium receptor was reported to bind halide anions based on $(C-H)^+...X$ hydrogen bonding, which has been studied in comparison with many other types of hydrogen bonding.[17] Furthermore, a modified tripodal imidazolium receptor[18] was synthesized by introducing a nitro group to the imidazolium sidearm to utilize charge−charge and charge−dipole interactions[19] showing enhanced anion affinity for chloride.

The incorporation of fluorescent chromophores into the receptor that are sensitive to interactions between the host and guest molecules has recently gained considerable attention because of their high sensitivity and low detection limit.[20,21] The appeal of fluorescent sensors originates from the high sensitivity of fluorescence detection compared to other spectroscopic methods. When a guest species binds to the fluorescent receptor, a certain property such as fluorescent intensity, wavelength, lifetime, etc. changes, and such a change serves as an indicator of guest binding. On account of its simplicity and high sensitivity, fluorescence is becoming of increasing importance for chemical trace detection. The linkage of cation crown ethers with fluorescent dyes[22] provides a novel method for monitoring low concentrations of alkali and alkaline earth metals, and in this connection, considerable effort has been devoted to developing fluorescent chemosensors for cations and neutral guests.[23] However, anion-selective receptors based on fluorescent chromophores have just begun to be investigated.[24,25] Inspite of the importance of fluoride receptor, there is a paucity of reports regarding a selective fluorescent sensor for fluoride ions, though some receptor compounds for fluoride ions have been reported.[26−28]

In this paper, we present a fluoride selective fluorescent as well as chromogenic chemosensor **1**, based on a naphthalene urea derivative, which shows a unique fluorescence and absorption peak in the presence of fluoride ions, and shed light on the binding nature of the receptor with fluoride by both experimental and theoretical studies.

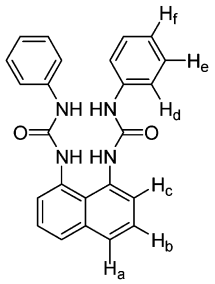

1

Experimental Section

1,8-Bis(*N*-phenylureido)naphthalene (1). To a solution of 0.2 g (1.3 mmol) 1,8-diaminonaphthalene in a 30 mL solution of THF and DMF (2:1 ratio) was slowly added 0.55 mL of phenylisocyanate (5.2 mmol) in 15 mL of THF over 30 min and refluxed for 4 h in a nitrogen atmosphere. The solid product was collected by filtration and washed with acetone

(10) Sessler, J. L.; Anzenbacher, P., Jr.; Jursíková, K.; Miyaji, H.; Genge, J. W.; Tvermoes, N. A.; Allen, W. E.; Shriver, J. A.; Gale, P. A. *Pure Appl. Chem*. **1998**, *70*, 2401.

(11) (a) Anzenbacher, P., Jr.; Jursíková, K.; Lynch, V. M.; Gale, P. A.; Sessler. J. L. *J. Am. Chem. Soc*. **1999**, *121*, 11020. (b) Miyaji, H.; Sato, W.; Sessler, J. L. *Angew. Chem., Int. Ed*. **2000**, *39*, 1777. (c) Anzenbacher, P., Jr.; Jursíková, K.; Shriver, J. A.; Miyaji, H.; Lynch, V. M.; Sessler, J. L.; Gale, P. A. *J. Org. Chem*. **2000**, *65*, 7641.

(12) Black, C. B.; Andrioletti, B.; Try, A. C.; Ruiperez, C.; Sessler, J. L. *J. Am. Chem. Soc*. **1999**, *121*, 10439.

(13) Mizuno, T.; Wei, W.-H.; Eller, L. R.; Sessler, J. L. *J. Am. Chem. Soc*. **2002**, *124*, 1134.

(14) Woods, C. J.; Camiolo, S.; Light, M. E.; Coles, S. J.; Hursthouse, M. B.; King, M. A.; Gale, P. A.; Essex, J. W. *J. Am. Chem. Soc*. **2002**, *124*, 8644.

(15) Mascal, M.; Armstrong, A.; Bartberger, M. D. *J. Am. Chem. Soc*. **2002**, *124*, 6274.

(16) Sato, K.; Arai, S.; Yamagishi, T. *Tetrahedron Lett*. **1999**, *40*, 5219.

(17) (a) Kim, K. S.; Tarakeshwar, P.; Lee, J. Y. *Chem. Rev*. **2000**, *100*, 4145. (b) Oh, K. S.; Cha, S.-S.; Kim, D.-H.; Cho, H.-S.; Ha, N.-C.; Choi, G.; Lee, J. Y.; Tarakeshwar, P.; Son, H. S.; Choi, K. Y.; Oh, B.-H.; Kim, K. S. *Biochemistry* **2000**, *39*, 13891. (c) Kim, K. S.; Oh, K. S.; Lee, J. Y. *Proc. Natl. Acad. Sci. USA* **2000**, *97*, 6373. (d) Tarakeshwar, P.; Choi, H. S.; Kim, K. S. *J. Am. Chem. Soc*. **2001**, *123*, 3323. (e) Kim, K. S.; Kim, D.; Lee, J. Y.; Tarakeshwar, P.; Oh, K. S. *Biochemistry* **2002**, *41*, 5300.

(18) Ihm, H.; Yun, S.; Kim, H. G.; Kim, J. K.; Kim, K. S. *Org. Lett*. **2002**, *4*, 2897.

(19) Cui, C.; Cho, S. J.; Kim, K. S. *J. Phys. Chem. A* **1998**, *102*, 1119.

(20) Keefe, M. H.; Benkstein, K. D.; Hupp, J. T. *Coord. Chem. Rev*. **2000**, *205*, 201.

(21) (a) Sun, S.-S.; Lees, A. J.; Zavalij, P. Y. *Inorg. Chem*. **2003**, *42*, 3445. (b) Charbonnière, L. J.; Ziessel, R.; Montalti, M.; Prodi, L.; Zaccheroni, N.; Boehme, C.; Wipff, G. *J. Am. Chem. Soc*. **200**2, *124*, 7779. (c) Anzenbacher, P., Jr.; Tyson, D. S.; Jursíková, K.; Castellano, F. N. *J. Am. Chem. Soc*. **2002**, *124*, 6232. (d) Watanabe, S.; Onogawa, O.; Komatsu, Y.; Yoshida, K. *J. Am. Chem. Soc*. **1998**, *120*, 229.

(22) Lohr, H. G.; Vogtle, F. *Acc. Chem. Res*. **1985**, *18*, 65.

(23) (a) Czarnik A. W. *Acc. Chem. Res*. **1994**, *27*, 302. (b) De Silva, A. P.; Gunaratne, H. Q. N.; Gunnlaugsson, T.; Huxley, A. T. M.; McCoy, C. P.; Rademacher, J. T.; Rice, T. E. *Chem. Rev*. **1997**, *97*, 1515. (c) Prodi, L.; Bolletta, F.; Montalti, M.; Zaccheroni, N. *Coord. Chem. Rev*. **2000**, *205*, 59.

(24) (a) Gunnlaugsson, T.; Davis, A. P.; O'Brien, J. E.; Glynn, M. *Org. Lett*. **2002**, *4*, 2449 and references therein. (b) Gunnlaugsson, T.; Davis, A. P.; Glynn, M. *Chem. Commun*. **2001**, 2556. (c) Nishizawa, S.; Kaneda, H.; Uchida, T.; Teramae, N. *J. Chem. Soc., Perkin Trans. 2* **1998**, 2325. (d) Fabbrizzi, L.; Faravelli, H.; Francese, G.; Licchelli, M.; Perotti, A.; Taglietti, A. *Chem. Commun*. **1998**, 971. (e) Wu, F.-Y.; Li, Z.; Wen, Z.-C.; Zhou, N.; Zhao, Y.-F.; Jiang, Y,-B. *Org. Lett*. **2002**, *4*, 3203. (f) Causey, C. P.; Allen, W. E. *J. Org. Chem*. **2002**, *67*, 5963. (g) Huston, M. E.; Akkaya, E. U.; Czarnik, A. W. *J. Am. Chem. Soc*. **1989**, *111*, 8735. (h) Vance, D. H.; Czarnik, A. W. *J. Am. Chem. Soc*. **1994**, *116*, 9397.

(25) (a) Miyaji, H.; Anzenbacher, Jr. P.; Sessler, J. L.; Bleasdale, E. R.; Gale, P. A. *Chem. Commun*. **1999**, 1723. (b) Anzenbacher, P., Jr.; Jursíková, K.; Sessler, J. L. *J. Am. Chem. Soc*. **2000**, *122*, 9350. (c) Cooper, C. R.; Spencer, N.; James, T. D. *Chem. Commun*. **1998**, 1365. (d) Kim, S. K.; Yoon, J. *Chem. Commun*. **2002**, 770.

(26) Cho, E. J.; Moon, J. W.; Ko, S. W.; Lee, J. Y.; Kim, S. K.; Yoon, J.; Nam, K. C. *J. Am. Chem. Soc*. **2003**, *125*, 12376.

(27) Lee, D. H.; Im, J. H.; Lee, J. H.; Hong, H. I. *Tetrahedron Lett*. **2002**, *43*, 9637.

(28) (a) Miyaji, H.; Anzenbacher, P., Jr.; Sessler, J. L.; Bleasdale, E. R.; Gale, P. A. *Chem. Commun*. **1999**, 1723. (b) Anzenbacher, P., Jr.; Jursíková, K.; Sessler, J. L. *J. Am. Chem. Soc*. **2000**, *122*, 9350.

to yield 0.37 g (75%) of **1**: mp 190−192 °C, dec; ^{1}H NMR (DMSO-d_6) δ 9.01 (s, 2H, NH), 8.85 (s, 2H, NH), 7.70 (two d, 4H, J = 7.5 Hz, ArH), 7.46 (dd, 2H, J = 7.5 Hz, ArH), 7.41 (d, 4H, J = 7.5 Hz, ArH), 7.22 (dd, 4H, J = 7.5 Hz, ArH), 6.92 (t, 2H, J = 7.5 Hz, ArH); ^{13}C NMR (DMSO-d_6) δ 153.5 (−CO), 140.1, 135.8, 134.1, 128.8, 125.6, 125.2, 122.5, 121.8, 118.5, 114.0 (Ar); FAB MS *m*/*z* 397 (M + 1, calcd 397). Anal. Calcd for $C_{24}H_{20}N_4O_2$: C, 72.73; H, 5.05; N, 14.14. Found: C, 72.68; H, 5.10; N, 14.10.

UV−Vis and Fluorescence Spectra. UV−vis experiments were carried out in the acetonitrile−DMSO (1:1, v/v) solution. A receptor solution (3×10^{-5} M) was titrated by addition of aliquots of fluoride anion solution (1.5×10^{-5} to 3×10^{-3} M) prepared by stock solution of the receptor. Fluorescence experiments (6 μM solution of receptor) were carried out in an acetonitrile−DMSO (9:1, v/v) solution with an excitation wavelength of 310 nm. Association constants were obtained using the computer program ENZFITTER, available from Elsevier-BIOSOFT, Cambridge, UK.

Calculational Methods. Three molecular complexes of **1** with halides (X^- = F^-, Cl^-, and Br^-) as well as **1** were optimized by density functional theory (DFT) calculations using the nonlocal density function of Becke's three parameters employing the Lee−Yang−Parr functional (B3LYP) with 6-31G* basis sets using the Gaussian 98 program suite.[29] The interaction energy is simply obtained by the energy of the complex subtracted by the sum of energies of constituents. Generally, basis set superposition error (BSSE) correction should be included to obtain an accurate interaction energy.[30] However, in this study, the interaction is very strong due to charged hydrogen bonding. Thus, the BSSE is expected to be negligible compared with the magnitude of the total interaction energies.

NMR shielding tensors were computed with the Gauge-Independent Atomic Orbital (GIAO) method.[31] Currently available functionals do not include a magnetic field dependence, so DFT methods do not provide systematically better NMR results than Hartree−Fock (HF).[32] Therefore, the chemical shifts were calculated at the HF level with the 6-31G* basis set at the B3LYP/6-31G*-optimized geometries.

The absorption spectra of **1**, its deprotonated form (**1**$^-$), and its complex with fluoride (**1F**$^-$) were simulated to look into the nature of interactions between **1** and fluoride. The absorbance is directly connected to the imaginary part of polarizability;[33] thus, we have only to obtain frequency-dependent polarizability. To this end, we have used the collective electronic oscillator (CEO) method, which was originally developed by Mukamel[34] and has been applied to various molecular systems.[35−39] Our calculations used the INDO/S semiempirical Hamiltonian, which was constructed to reproduce the spectra of simple molecules at the singly excited CI level. This Hamiltonian, introduced by Pople[40] and parametrized by Zerner and collaborators,[41] is widely used in optical response computations. We first carried out geometry optimization by ab initio DFT or semiempirical AM1 calculations and then solved time-dependent Hartree−Fock (TDHF) equations[42] of motion for the density matrix in Liouville space to obtain the frequency-dependent polarizability. Detailed theoretical backgrounds and procedures are available elsewhere.[43]

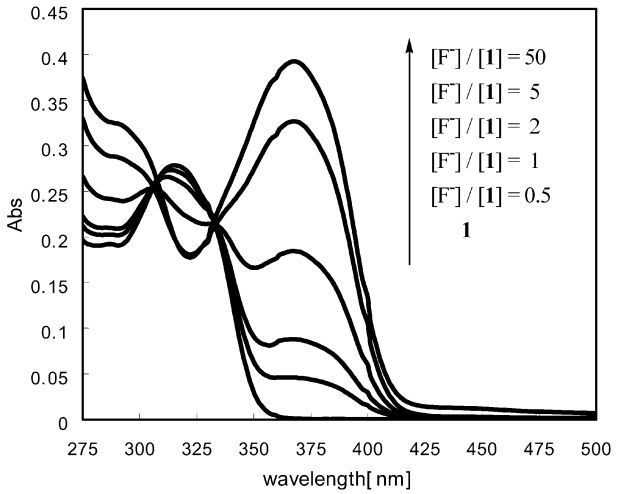

FIGURE 1. UV−vis spectra of solutions containing **1** (3×10^{-5} M) and fluoride ion in acetonitrile−DMSO (1:1, v/v).

Results and Discussion

Our host **1** displays a unique new peak around 370 nm upon the addition of fluoride in its absorption spectra as shown in Figure 1. Without the fluoride anion, the absorption peak appears at 315 nm, which gradually decreases and finally disappears as the concentration of fluoride anion increases. The fluorescence study in acetonitrile−DMSO (9:1) shows the same tendency, that is, the unique peak at 445 nm appears and the intensity of

(29) Frisch, M. J.; Trucks, G. W.; Schlegel, H. B.; Scuseria, G. E.; Robb, M. A.; Cheeseman, J. R.; Zakrzewski, V. G.; Montgomery, J. A., Jr.; Stratmann, R. E.; Burant, J. C.; Dapprich, S.; Millam, J. M.; Daniels, A. D.; Kudin, K. N.; Strain, M. C.; Farkas, O.; Tomasi, J.; Barone, V.; Cossi, M.; Cammi, R.; Mennucci, B.; Pomelli, C.; Adamo, C.; Clifford, S.; Ochterski, J.; Petersson, G. A.; Ayala, P. Y.; Cui, Q.; Morokuma, K.; Malick, D. K.; Rabuck, A. D.; Raghavachari, K.; Foresman, J. B.; Cioslowski, J.; Ortiz, J. V.; Stefanov, B. B.; Liu, G.; Liashenko, A.; Piskorz, P.; Komaromi, I.; Gomperts, R.; Martin, R. L.; Fox, D. J.; Keith, T.; Al-Laham, M. A.; Peng, C. Y.; Nanayakkara, A.; Gonzalez, C.; Challacombe, M.; Gill, P. M. W.; Johnson, B. G.; Chen, W.; Wong, M. W.; Andres, J. L.; Head-Gordon, M.; Replogle, E. S.; Pople, J. A. *Gaussian 98*, revision A.6; Gaussian, Inc.: Pittsburgh, PA, 1998.

(30) (a) Jansen, H. B.; Ros, P. *Chem. Phys. Lett.* **1969**, *3*, 140. (b) Boys, S. F.; Bernardi, F. *Mol. Phys.* **1970**, *19*, 553.

(31) (a) Wolinski, K.; Hilton, J. F.; Pulay, P. *J. Am. Chem. Soc.* **1990**, *112*, 8251. (b) Dodds, J. L.; McWeeny, R.; Sadlej, A. J. *Mol. Phys.* **1980**, *41*, 1419. (c) McWeeny, *Phys. Rev.* **1962**, *126*, 1028. (d) Ditchfield, R. *Mol. Phys.* **1974**, *27*, 789.

(32) Frish, A.; Frisch, M. J. *Gaussian 98 User's Reference*; Gaussian, Inc. Pittsburgh, PA., 1998.

(33) Mukamel, S. *Principles of Nonlinear Optical Spectroscopy*; Oxford University Press: New York, 1995.

(34) (a) Mukamel, S.; Wang, H. X. *Phys. Rev. Lett.* **1992**, *69*, 65. (b) Mukamel, S.; Takahashi, A.; Wang, H. X.; Chen, G. *Science* **1994**, *266*, 250. (c) Takahashi, A.; Mukamel, S. *J. Chem. Phys.* **1994**, *100*, 2366.

(35) Mukamel, S.; Tretiak, S.; Wagersreiter, T.; Chernyak, V. *Science* **1997**, *277*, 781.

(36) (a) Tretiak, S.; Chernyak, V.; Mukamel, S. *J. Phys. Chem. B* **1998**, *102*, 3310. (b) Tretiak, S.; Middleton, C.; Chernyak, V.; Mukamel, S. *J. Phys. Chem. B* **2000**, *104*, 4519. (c) Tretiak, S.; Chernyak, V.; Mukamel, S. *J. Am. Chem. Soc.* **1997**, *119*, 11408.

(37) (a) Tretiak, S.; Middleton, C.; Chernyak, V.; Mukamel, S. *J. Phys. Chem. B* **2000**, *104*, 9540. (b) Tretiak, S.; Saxena, A.; Martin, R. L.; Bishop, A. R. *J. Phys. Chem. B* **2000**, *104*, 7029. (c) Tretiak, S.; Chernyak, V.; Mukamel, S. *Chem. Phys. Lett.* **1996**, *259*, 55.

(38) (a) Toury, T.; Zyss, J.; Chernyak, V.; Mukamel, S. *J. Phys. Chem. B* **2001**, *105*, 5692. (b) Chernyak, V.; Schultz, M. F.; Mukamel, S.; Tretiak, S.; Tsiper, E. V. *J. Chem. Phys.* **2000**, *113*, 36.

(39) (a) Bazan, G. C.; Oldham, W. J., Jr.; Lachicotte, R. J.; Tretiak, S.; Chernyak, V.; Mukamel, S. *J. Am. Chem. Soc.* **1998**, *120*, 9188. (b) Zyss, J.; Ledoux, I.; Volkov, S.; Chernyak, V.; Mukamel, S.; Bartholomew, G. P.; Bazan, G. C. *J. Am. Chem. Soc.* **2000**, *122*, 11956. (c) Tertiak, S.; Chernyak, V.; Mukamel, S. *Int. J. Quant. Chem.* **1998**, *70*, 711.

(40) (a) Pople, J. A.; Segal, G. A. *J. Chem. Phys.* **1965**, *43*, S136. (b) Pople, J. A.; Beveridge, D. L.; Dobosh, P. *J. Chem. Phys.* **1967**, *47*, 2026.

(41) (a) Ridley, J.; Zerner, M. C. *Theor. Chim. Acta.* **1973**, *32*, 111. (b) Zerner, M. C.; Loew, G. H.; Kirchner, R. F.; Mueller-Westerhoff, U. T. *J. Am. Chem. Soc.* **1980**, *102*, 589. (c) Bacon, A. D.; Zerner, M. C. *Theor. Chim. Acta.* **1979**, *53*, 21.

(42) Dirac, P. A. *Proc. Camb. Philos. Soc.* **1930**, *26*, 376.

(43) Tretiak, S.; Mukamel, S. *Chem. Rev.* **2002**, *102*, 3171 and references therein.

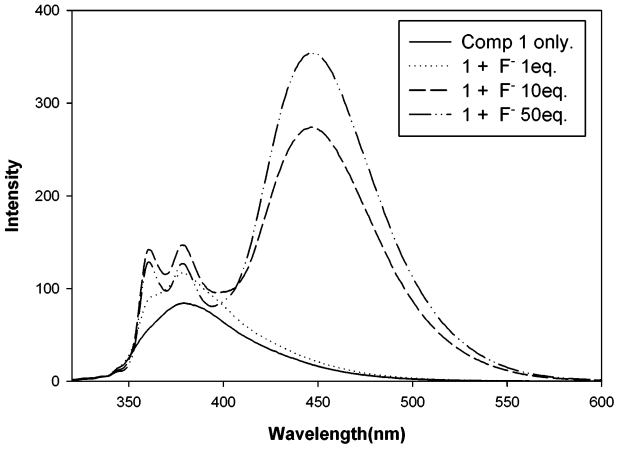

FIGURE 2. Fluorescence changes of **1** (6 μM) upon the addition of tetrabutylammonium fluoride in acetonitrile−DMSO (9:1, v/v) (excitation wavelength = 310 nm).

the peak at 379 nm decreases.[26] On the other hand, it has been found that the new fluorescence peak at 445 nm does not appear in the presence of chloride, bromide, or iodide anions.[26] From the fluorescence titration experiments, the association constants for fluoride and chloride were calculated to be 14200 and 380 M^{-1}, respectively, with errors less than 10%. The selectivity for fluoride is almost 40-fold greater than that for chloride. The selectivity for fluoride is not that high; however, the new peak in the presence of fluoride could give a great advantage for detecting fluoride anions.

Figure 2 shows the changes of fluorescent emission of **1** in the presence of fluoride anion (refer to ref 26 for other halides). Without the fluoride anion, the fluorescence peak appears at 379 nm, while in the presence of 50 equiv of fluoride anion, the peak appears at 448 nm. The red shift of fluorescence emission is connected with the red shift of absorption peak in the presence of fluoride, since the emission energy is lowered as the excitation energy is lowered.

To elucidate the intermolecular interactions between the host molecule and fluoride anion, we also carried out ^{1}H NMR titration experiments in DMSO-d_6 and ab initio calculations to obtain energy minimum structures, binding energies, and NMR chemical shifts and compared the results. Figure 3 shows the experimentally and theoretically obtained NMR spectra of **1** and its complex with fluoride (**1F**$^-$). The experimental NMR spectrum of **1** shows characteristic peaks of eight protons as assigned. The NMR spectrum of **1F**$^-$, which was obtained in the presence of 100 equiv of fluoride anion, shows dramatic changes in those proton peaks. In the presence of fluoride anion, two amide N−H signals disappear rapidly, and aromatic proton (H_a through H_f) signals shift downfield or upfield due to the interactions between **1** and fluoride anion. The amide N−H signals disppeared. H_c and H_d protons at the ortho position of the urea group show a moderate downfield shift of $\Delta\delta$ = +0.35 and +0.44 ppm, respectively, upon addition of fluoride anions due to the hydrogen bond between H_c/H_d and urea oxygen when the fluoride anion binds with four urea N−H protons. On the other hand, H_a shows a significan peak shifted upfield by $\Delta\delta$ = −0.88 ppm, while slight upfield shifts are observed for H_b, H_e, and H_f of $\Delta\delta$ = −0.45, −0.14, and −0.28 ppm, respectively. The upfield shifts of H_a and H_f protons can be understood from the enhanced resonance of naphthalene as well as phenyl electrons from the anionic character of urea nitrogen, which will be discussed later in detail. In the simulated ^{1}H NMR spectrum in the presence of fluoride anion, the changes of proton signals ($\Delta\delta$) for H_a, H_b, H_c, H_d, H_e, and H_f are −0.74, −0.35, 0.71, −0.36, −0.47, and −0.62 ppm, respectively. The calculated ^{1}H NMR spectra of **1** and **1F**$^-$ are in good agreement with the spectra obtained experimentally except that the simulated H_d signal, in the presence of fluoride anion, is shifted upfield compared with that in the absence of fluoride anion, while it is shifted downfield in the experimental spectrum. The correlation spectrum of two-dimensional COSY indicates that H_a and H_c are correlated with H_b, while H_d and H_f are correlated with H_e.[26]

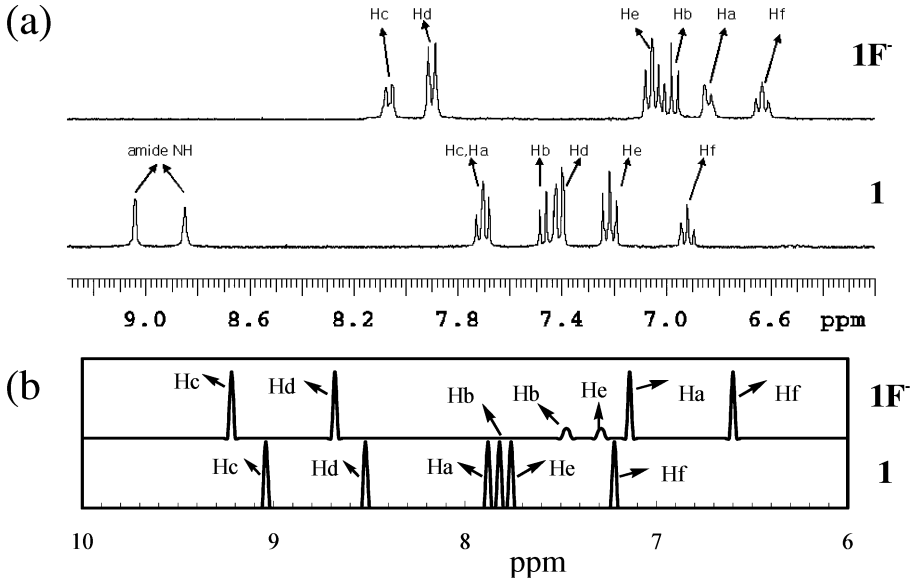

FIGURE 3. Experimental (a) and simulated (b) NMR spectra of **1** and **1F**$^-$.

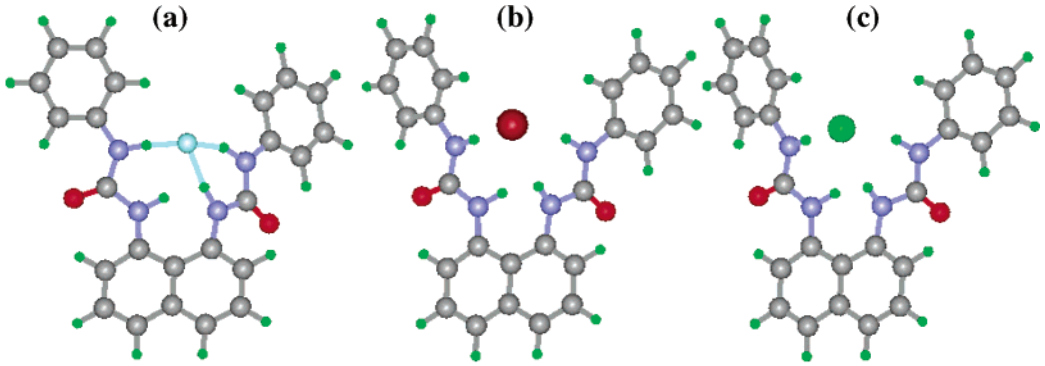

FIGURE 4. B3LYP/6-31G*-predicted optimized structures of complexes of **1** with fluoride (a), chloride (b), and bromide (c).

The B3LYP/6-31G*-optimized structures for the complexes of receptor with halides (F^-, Cl^-, Br^-) are represented in Figure 3. The interaction energies without basis set superposition error correction are −128.7, −56.1, and −55.6 kcal/mol for F^-, Cl^-, and Br^-, respectively. The large binding energy difference between F^- and Cl^-/Br^- may result in the binding selectivity for F^- over Cl^-/Br^-, as is observed in the fluorescence titration experiment. The binding energy comes from the strongly charged hydrogen bonding between halide anion and four amide protons. It should be noted that one of the amide protons (near the naphthalene rather than benzene) does form an intramolecular hydrogen bond with the opposite amide nitrogen atom as shown in Figure 4. The interatomic distances between halide anion and three amide protons (which do not involve an intramolecular hydrogen bond) are 1.61, 1.54, and 1.67 Å for fluoride, 2.20, 2.25, and 2.31 Å for chloride, and 2.35, 2.43, and 2.45 Å for bromide. The fluoride is smaller and harder than chloride and bromide, and it can approach much closer toward the cavity, which is surrounded by four amide protons and has a measure of positive electrostatic potential. It is interesting to note that the interatomic distances for chloride and bromide are not so different; hence, the hydrogen bonding energies are predicted to be similar. As a matter of fact, the calculated interaction energies are almost equivalent for chloride and bromide.

To understand the nature of UV spectral changes in the presence of fluoride, we simulated absorption spectra of **1**, its deprotonated form (**1**$^-$), and its complex with fluoride (**1F**$^-$) using CEO algorithm using the lowest 50 oscillators. Figure 5 displays the absorption spectra simulated with line width of 0.1 eV, which is a typical dephasing constant for conjugated organic molecules. We used the B3LYP/6-31G*-optimized geometries as an input for CEO calculations. Apparently, the absorption spectra seems to be different from those obtained using AM1-optimized geometries, which were published previously.[26] However, the peak at about 259 nm of **1F**$^-$ for B3LYP geometry corresponds to the peak at ∼240 nm for AM1 geometry. For both geometries, the spectra of **1** and **1**$^-$ are similar to each other. Of course, the degrees of red-shift are different for the two geometries. Thus, the results are not so much different. The reason the spectra seem to be quite different is that the spectra were shown in the range from 250 to 500 nm as the experiment showed. Around 250 nm, there are two peaks for **1F**$^-$ for B3LYP but only one peak for AM1. However, the AM1

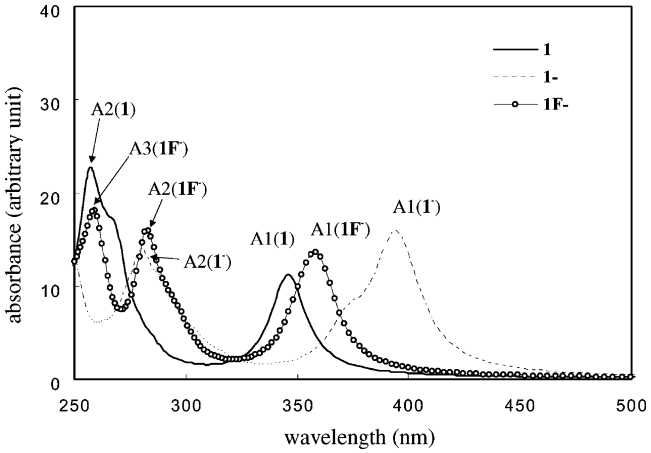

FIGURE 5. Simulated absorption spectra of **1**, **1**$^-$, and **1F**$^-$. See the text for the notation of band assignments.

geometry gives a peak at ∼240 nm, and this peak was not shown in the range from 250 to 500 nm in our previous paper.[26] In the absorption spectra, we denote the lowest energy (longest wavelength) peak as A1, and the next lowest one as A2, etc. Then, we define the molecule in the notation. For example, A1(**1**), A1(**1**$^-$), and A1(**1F**$^-$) denote the lowest energy absorption peaks for **1**, **1**$^-$, and **1F**$^-$, respectively, and A2(**1**), A2(**1**$^-$), and A2(**1F**$^-$) denote the second lowest energy absorption peaks for **1**, **1**$^-$, and **1F**$^-$, respectively, and so on. In the range of wavelengths from 250 to 500 nm, there are two absorption peaks for **1** and **1**$^-$, while there are three peaks for **1F**$^-$. The simulated lowest absorption peak appears at about 346 nm for **1**. When **1** forms a complex with **F**$^-$, the absorption peak at 346 nm disappears and appears at about 362 nm with a 16 nm red shift. On the other hand, we found that the peak appeared at 345 nm for **1** and was red-shifted by 63 nm in the presence of **F**$^-$ when we used AM1-optimized geometries. Several previous applications of CEO methods have shown that the CEO calculations using an INDO/S Hamiltonian with AM1-optimized geometries give reasonable absorption spectra.[39] More recently, the CEO methods with B3LYP/6-31G*-optimized structures was successfully applied to porphyrin systems.[44] There still remains a controversy over which level of calculations is best for optical transi-

(44) Nguyen, K. A.; Day, P. N.; Pachter, R.; Tretiak, S.; Chernyak, V.; Mukamel, S. *J. Phys. Chem. A* **2002**, *106*, 10285.

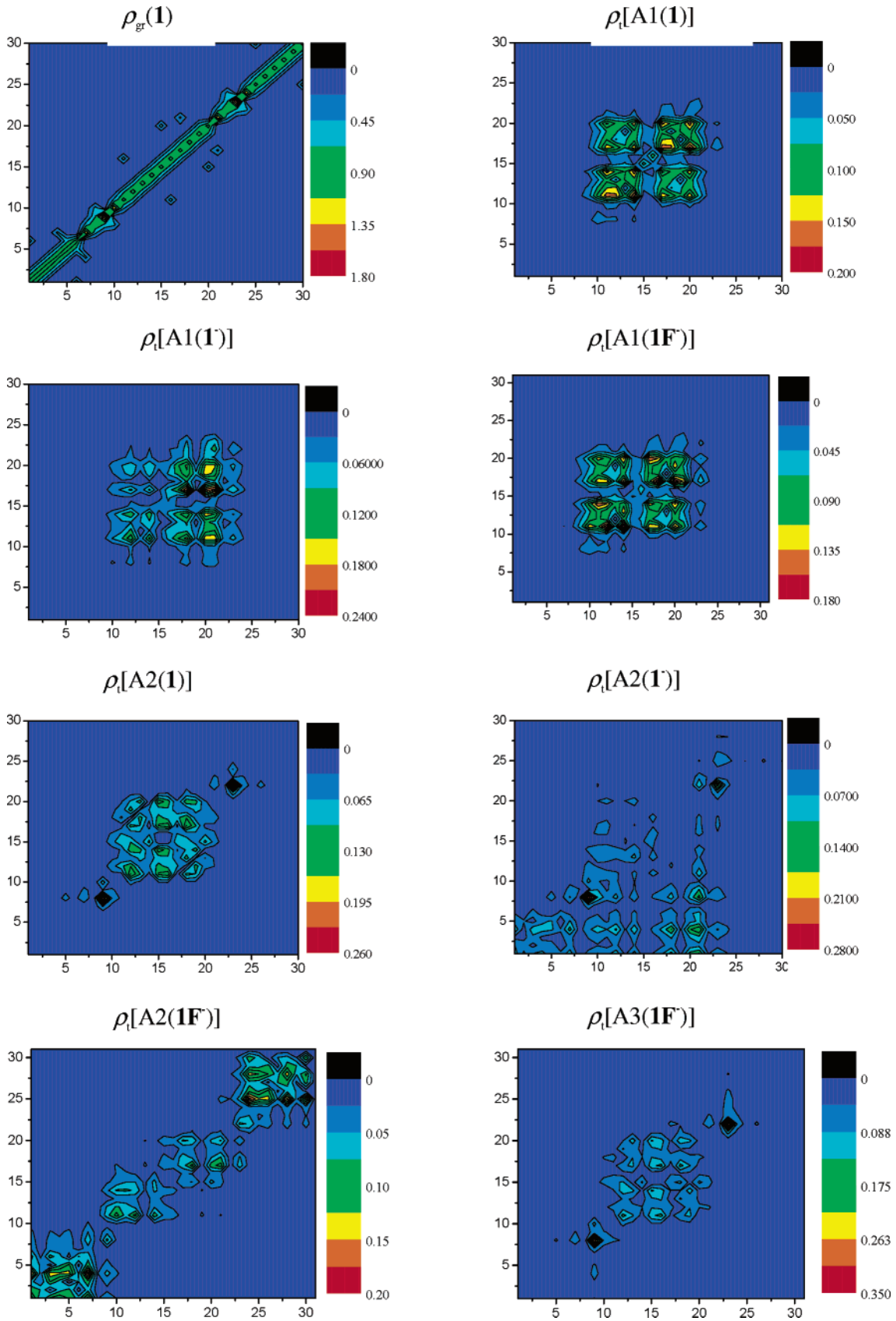

FIGURE 6. Contour maps of ground-state and transition density matrixes. See text for notations.

tion properties such as absorption spectra. It has been quite system dependent until now. As a matter of fact, the experimental absorption peak was red-shifted by 53 nm upon the addition of $\mathbf{F}^-$, and the AM1-optimized geometry gives better agreement with the experiment. From the comparison of absorption spectra of **1**, $\mathbf{1}^-$, and

SCHEME 1

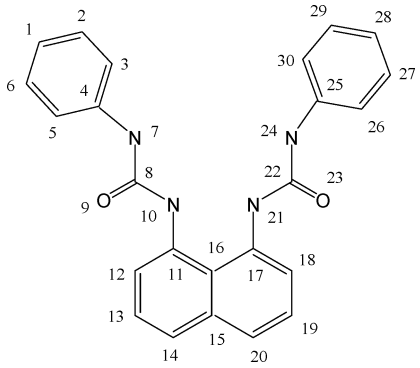

1F$^-$, it can be concluded that **1F**$^-$ has both neutral and anionic characteristics.

The transition density matrixes corresponding to the most contributing electronic oscillators to each absorption peaks have been investigated. It is interesting to find out some similarities and differences in the nature of corresponding transitions. The contour maps of the density matrix for the ground state of **1**, ρ_{gr}(**1**), and the transition density matrixes for the dominating oscillators to the corresponding absorptions (ρ_t[A1(**1**)], ρ_t[A2(**1**)], ρ_t[A1(**1**$^-$)], ρ_t[A2(**1**$^-$)], ρ_t[A1(**1F**$^-$)], ρ_t[A2(**1F**$^-$)], ρ_t[A3(**1F**$^-$)]) are depicted in Figure 6. To present the electron−hole coherences, the abscissa and ordinate represent the electron and hole axes, respectively, and the numbers show the atomic number as seen in the Scheme 1. We excluded the hydrogen atoms in the atomic numbering because the π electrons are responsible for the electronic transitions by UV light and hydrogen atoms do not carry π electrons. The diagonal elements (ρ_{mm}) of the ground-state density matrix represent the charges of mth atom, whereas the off-diagonal elements (ρ_{nm}) reflect the chemical bonding between nth and mth atoms. On the other hand, the diagonal (ρ_{mm}) and off-diagonal (ρ_{nm}) elements of the transition density matrix represent on-site and off-site electron−hole interactions, respectively, when the light with transition energy irradiates the molecule. The $\pi\rightarrow\pi^*$ transitions of the naphthalene are responsible for A1 for all three systems. For A1, off-site transition as well as on-site transition is also contributing as noted from the diagonal and off-diagonal elements of the corresponding transition density matrixes. Generally, a red-shifted absorption peak is observed when the chromophore is deprotonated at the atom directly connected to a chromophore. In our calculations, A1 peaks for **1**$^-$ and **1F**$^-$ show red-shifts of about 50 and 12 nm from that for **1**, respectively. Thus, **1F**$^-$ has some anionic characters, which results from the strongly charged anionic hydrogen bonding between fluoride and four amide protons. This is further supported by the transition density matrixes of higher energy absorption peaks. The absorption peaks of **1F**$^-$ at 283 and 259 nm are near the absorption peak (283 nm) of **1**$^-$ and the absorption peak (257 nm) of **1**, respectively, as seen in Figure 4. Very interestingly, the transition density matrix corresponding to A2(**1F**$^-$) is similar to that corresponding to A2(**1**$^-$), while the transition density matrix corresponding to A3(**1F**$^-$) is similar to that corresponding to A2(**1**). In other words, for the complex, the absorption peak at 283 nm has an anionic nature and the peak at 259 nm has a neutral nature.

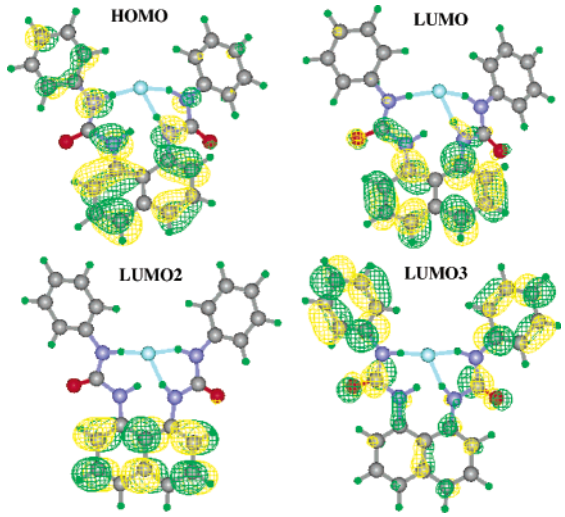

FIGURE 7. B3LYP/6-31G*-predicted highest occupied molecular orbital (HOMO), lowest unoccupied molecular orbital (LUMO), second LUMO (LUMO2), and third LUMO (LUMO3).

The transition density matrix corresponding to A2(**1**) (ρ_t[A2(**1**)]) shows a picture similar to ρ_t[A1(**1**)] except that the electron−hole interactions in the urea groups are also contributing to A2(**1**). The transition density matrix corresponding to A3(**1F**$^-$) (ρ_t[A3(**1F**$^-$)]) resembles ρ_t[A2(**1**)], as expected from the comparison of absorption peak positions. The ρ_t[A2(**1**$^-$)] shows that the electron−hole interactions are almost delocalized over the whole molecule, and the off-diagonal elements are asymmetric due to the fact that only one amide proton is removed. A similar transition density matrix is obtained in ρ_t[A2(**1F**$^-$)] with almost symmetric off-diagonal elements.

The highest occupied molecular orbital (HOMO) and three lowest unoccupied molecular orbitals (LUMOs) of **1F**$^-$ were drawn in Figure 7. The HOMO electrons transfer to the LUMOs when **1F**$^-$ absorbs UV light. From the molecular orbitals, it should be noted that the electron−hole interactions (which can be considered as occupied orbital−unoccupied orbital interactions) of the naphthalene and other parts are important to the electronic transitions. The transitions from HOMO to LUMO and LUMO2 can be assigned as A1(**1F**$^-$) and A3(**1F**$^-$), respectively. For these transitions, the electron−hole interactions are only focused on the naphthalene, which is consistent with our previous discussion based on the transition density matrixes. On the other hand, the transition from HOMO to LUMO3 can be assigned as A2(**1F**$^-$), where the electron−hole interactions are extended over the whole molecule.

Conclusion

Two phenylurea groups were introduced at the 1,8-position of naphthalene in our system. The naphthalene moiety acts as a fluorescent source and the urea group as a template for introducing the binding selectivity. Naphthalene urea derivative **1** displays selective fluorescent effects with fluoride ions in acetonitrile−DMSO. The binding selectivity of **1** for fluoride ions was as high as 40 times that for chloride ions with a new fluorescence peak at 445 nm; hence, **1** can be used as an efficient

fluoride sensor. The simulated ^{1}H NMR spectra of **1** and **1F**$^-$ are in good agreement with experimental spectra, and could give a reasonable explanation for the fluorescence changes of **1** upon the addition of fluoride anion. The calculated structures, energies, and absorption spectra support that the molecule **1** binds with fluoride anion by strongly charged hydrogen bonding between fluoride and amide NH groups. The binding selectivity for fluoride results from the fact that the small fluoride ion can fit into a small pocket surrounded by four amide protons. It is found from the transition density matrixes and MO pictures that **1F**$^-$ has both anionic and neutral characteristics. This compound has potential for practical application and is currently being investigated.

Acknowledgment. This research was supported by a Grant (No. KRF-2003-042-C00044) of Cooperative Research Project from Korea Research Foundation.

Supporting Information Available: The energies of F^-, Cl^-, Br^-, 1, $1F^-$, $1Cl^-$, and $1Br^-$, the number of imaginary frequencies of 1 and $1F^-$, and Cartesian coordinates of 1, $1F^-$, $1Cl^-$, and $1Br^-$. This material is available free of charge via the Internet at http://pubs.acs.org.

JO0356457